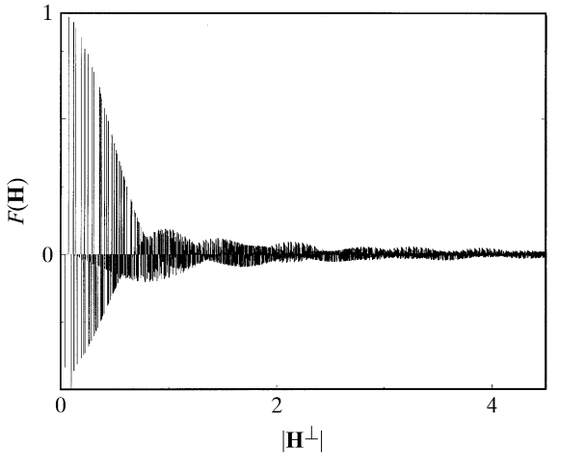

Fig. 4.6.3.22. Radial distribution function of the structure factors $F(\mathbf{H})$ of the Penrose tiling (edge length of the Penrose unit rhombs a_r = 4.04 Å) decorated with point atoms as a function of $\mathbf{H}^{\perp}$. All structure factors within $10^{-4}|F(\mathbf{0})|^2 < |F(\mathbf{H})|^2 < |F(\mathbf{0})|^2$ and $0 \leq |\mathbf{H}^{\parallel}| \leq 2.5$ Å^{-1} have been used and normalized to $F(0000) = 1$.

structure consisting of point atoms on the lattice nodes, the Bragg reflections show intensities depending on the perpendicular-space components of their diffraction vectors (Figs. 4.6.3.19, 4.6.3.20 and 4.6.3.22).

4.6.3.3.2.5. Relationships between structure factors at symmetry-related points of the Fourier image

Scaling the Penrose tiling by a factor τ^{-n} by employing the matrix S^{-n} scales at the same time its reciprocal space by a factor τ^n:

$$S\mathbf{H} = \begin{pmatrix} 0 & 1 & 0 & \bar{1} & 0 \\ 0 & 1 & 1 & \bar{1} & 0 \\ \bar{1} & 1 & 1 & 0 & 0 \\ \bar{1} & 0 & 1 & 0 & 0 \\ 0 & 0 & 0 & 0 & 1 \end{pmatrix}_D \begin{pmatrix} h_1 \\ h_2 \\ h_3 \\ h_4 \\ h_5 \end{pmatrix} = \begin{pmatrix} h_2 - h_4 \\ h_2 + h_3 - h_4 \\ -h_1 + h_2 + h_3 \\ -h_1 + h_3 \\ h_5 \end{pmatrix}.$$

Since this operation increases the lengths of the diffraction vectors by the factor τ in parallel space and decreases them by the factor $1/\tau$ in perpendicular space, the following distribution of structure-factor magnitudes (for point atoms at rest) is obtained:

$$\begin{aligned} |F(S^n\mathbf{H})| > |F(S^{n-1}\mathbf{H})| > \ldots > |F(S^1\mathbf{H})| > |F(\mathbf{H})|, \\ |F(\tau^n\mathbf{H}^{\parallel})| > |F(\tau^{n-1}\mathbf{H}^{\parallel})| > \ldots > |F(\tau\mathbf{H}^{\parallel})| > |F(\mathbf{H})|. \end{aligned}$$

The scaling operations S^n, $n \in \mathbb{Z}$, the rotoscaling operations $(\Gamma(\alpha)S^2)^n$ (Fig. 4.6.3.14) and the tenfold rotation $(\Gamma(\alpha))^n$, where

$$(\Gamma(\alpha)S^2)^n = \begin{pmatrix} 1 & 1 & \bar{1} & \bar{1} & 0 \\ 1 & 2 & 0 & \bar{2} & 0 \\ 0 & 2 & 1 & \bar{1} & 0 \\ \bar{1} & 1 & 1 & 0 & 0 \\ 0 & 0 & 0 & 0 & 1 \end{pmatrix}^n_D,$$

connect all structure factors with diffraction vectors pointing to the nodes of an infinite series of pentagrams. The structure factors with positive signs are predominantly on the vertices of the pentagram while the ones with negative signs are arranged on circles around the vertices (Figs. 4.6.3.24 to 4.6.3.27).

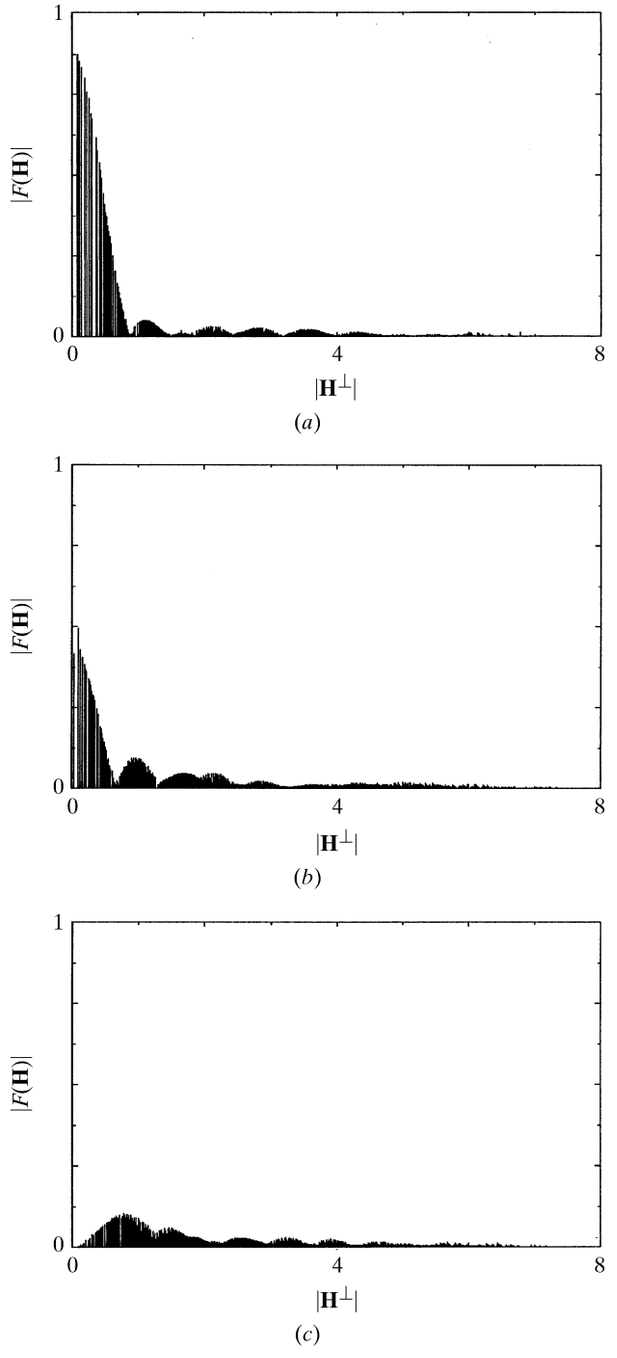

Fig. 4.6.3.23. Radial distribution function of the structure-factor magnitudes $|F(\mathbf{H})|$ of the Penrose tiling (edge length of the Penrose unit rhombs a_r = 4.04 Å) decorated with point atoms as a function of $\mathbf{H}^{\perp}$. All structure factors within $10^{-4}|F(\mathbf{0})|^2 < |F(\mathbf{H})|^2 < |F(\mathbf{0})|^2$ and $0 \leq |\mathbf{H}^{\parallel}| \leq 2.5$ Å^{-1} have been used and normalized to $F(0000) = 1$. The branches with (*a*) $|\sum_{i=1}^4 h_i| = 0 \bmod 5$, (*b*) $|\sum_{i=1}^4 h_i| = 1 \bmod 5$ and (*c*) $|\sum_{i=1}^4 h_i| = 2 \bmod 5$ are shown.

4.6.3.3.3. Icosahedral phases

A structure that is quasiperiodic in three dimensions and exhibits icosahedral diffraction symmetry is called an icosahedral phase. Its holohedral Laue symmetry group is $K = m\bar{3}\bar{5}$. All reciprocal-space vectors $\mathbf{H} = \sum_{i=1}^6 h_i\mathbf{a}_i^* \in M^*$ can be represented on a basis $\mathbf{a}_1^* = a^*(0, 0, 1)$, $\mathbf{a}_i^* = a^*[\sin\theta\cos(2\pi i/5), \sin\theta\sin(2\pi i/5), \cos\theta]$, $i = 2, \ldots, 6$ where $\sin\theta = 2/(5)^{1/2}$, $\cos\theta = 1/(5)^{1/2}$ and $\theta \simeq 63.44°$, the angle between two neighbouring fivefold axes (Fig. 4.6.3.28). This can be rewritten as

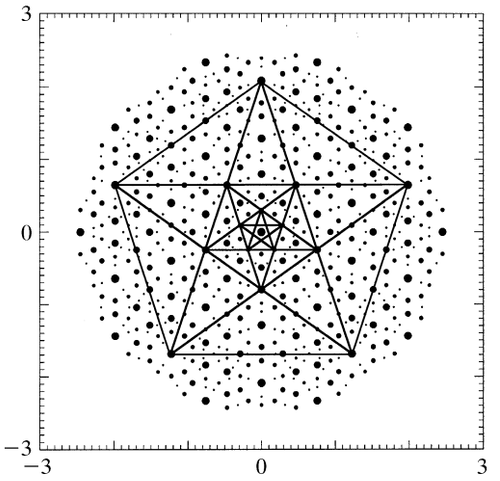

Fig. 4.6.3.24. Pentagrammal relationships between scaling symmetry-related positive structure factors $F(\mathbf{H})$ of the Penrose tiling (edge length $a_r = 4.04$ Å) in parallel space. The magnitudes of the structure factors are indicated by the diameters of the filled circles.

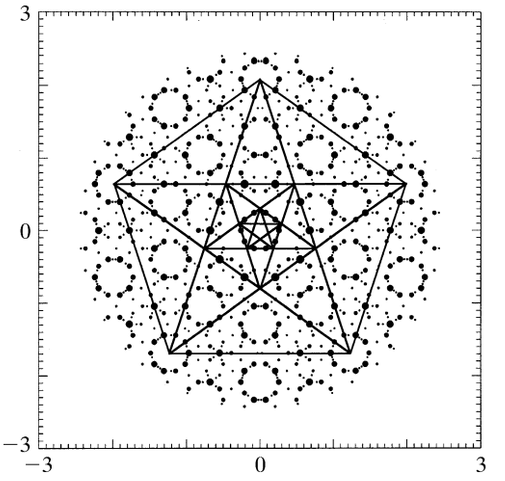

Fig. 4.6.3.25. Pentagrammal relationships between scaling symmetry-related negative structure factors $F(\mathbf{H})$ of the Penrose tiling (edge length $a_r = 4.04$ Å) in parallel space. The magnitudes of the structure factors are indicated by the diameters of the filled circles.

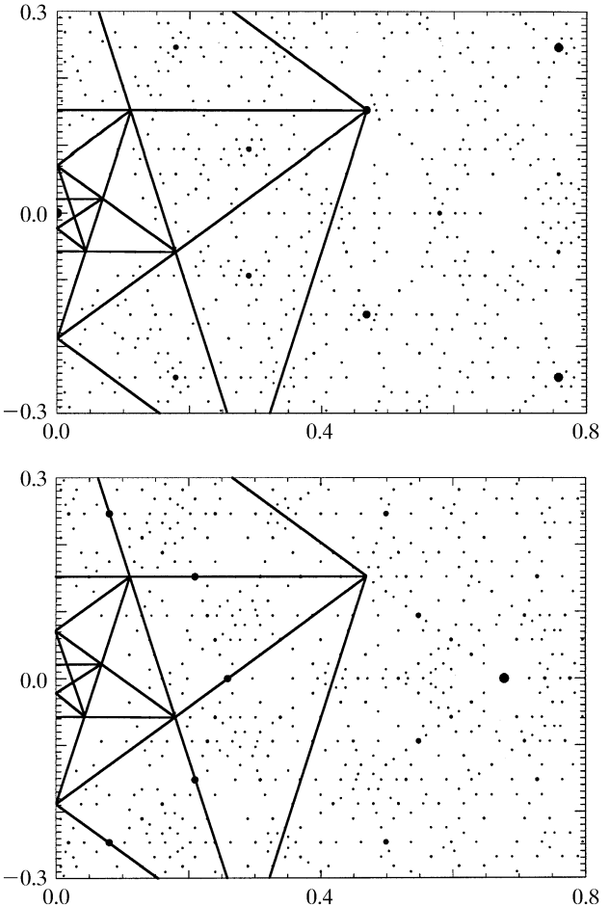

Fig. 4.6.3.26. Pentagrammal relationships between scaling symmetry-related structure factors $F(\mathbf{H})$ of the Penrose tiling (edge length $a_r = 4.04$ Å) in parallel space. Enlarged sections of Figs. 4.6.3.24 (above) and 4.6.3.25 (below) are shown.

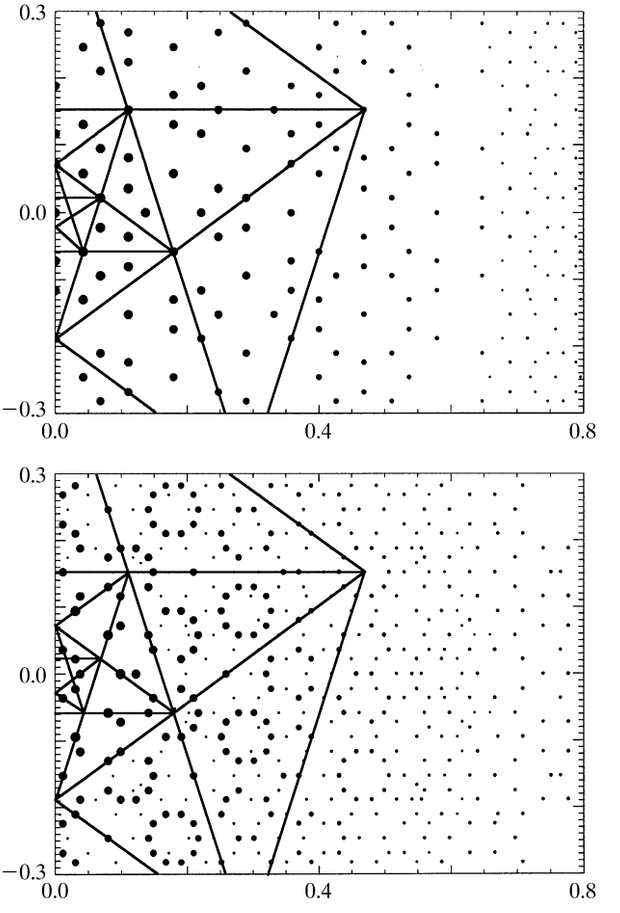

Fig. 4.6.3.27. Pentagrammal relationships between scaling symmetry-related structure factors $F(\mathbf{H})$ of the Penrose tiling (edge length $a_r = 4.04$ Å) in perpendicular space. Enlarged sections of positive (above) and negative structure factors (below) are shown.

$$\begin{pmatrix} \mathbf{a}_1^* \\ \mathbf{a}_2^* \\ \mathbf{a}_3^* \\ \mathbf{a}_4^* \\ \mathbf{a}_5^* \\ \mathbf{a}_6^* \end{pmatrix} = a^* \begin{pmatrix} 0 & 0 & 1 \\ \sin\theta\cos(4\pi/5) & \sin\theta\sin(4\pi/5) & \cos\theta \\ \sin\theta\cos(6\pi/5) & \sin\theta\sin(6\pi/5) & \cos\theta \\ \sin\theta\cos(8\pi/5) & \sin\theta\sin(8\pi/5) & \cos\theta \\ \sin\theta & 0 & \cos\theta \\ \sin\theta\cos(2\pi/5) & \sin\theta\sin(2\pi/5) & \cos\theta \end{pmatrix} \begin{pmatrix} \mathbf{e}_1^V \\ \mathbf{e}_2^V \\ \mathbf{e}_3^V \end{pmatrix},$$

where $\mathbf{e}_i^V$ are Cartesian basis vectors. Thus, from the number of independent reciprocal-basis vectors needed to index the Bragg reflections with integer numbers, the dimension of the embedding space has to be six. The vector components refer to a Cartesian coordinate system (V basis) in the physical (parallel) space.

The set $M^* = \{\mathbf{H}^{\parallel} = \sum_{i=1}^{6} h_i \mathbf{a}_i^* | h_i \in \mathbb{Z}\}$ of all diffraction vectors remains invariant under the action of the symmetry operators of the icosahedral point group $K = m\bar{3}\bar{5}$. The symmetry-adapted matrix representations for the point-group generators, one five-

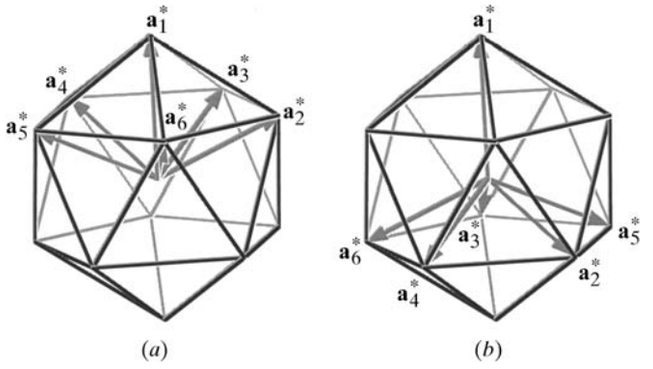

Fig. 4.6.3.28. Perspective (*a*) parallel- and (*b*) perpendicular-space views of the reciprocal basis of the 3D Penrose tiling. The six rationally independent vectors $\mathbf{a}_i^*$ point to the edges of an icosahedron.

fold rotation α, a threefold rotation β and the inversion operation γ, can be written in the form

$$\Gamma(\alpha) = \begin{pmatrix} 1 & 0 & 0 & 0 & 0 & 0 \\ 0 & 0 & 0 & 0 & 0 & 1 \\ 0 & 1 & 0 & 0 & 0 & 0 \\ 0 & 0 & 1 & 0 & 0 & 0 \\ 0 & 0 & 0 & 1 & 0 & 0 \\ 0 & 0 & 0 & 0 & 1 & 0 \end{pmatrix}_D, \Gamma(\beta) = \begin{pmatrix} 0 & 1 & 0 & 0 & 0 & 0 \\ 0 & 0 & 0 & 0 & 0 & 1 \\ 0 & 0 & 0 & \bar{1} & 0 & 0 \\ 0 & 0 & 0 & 0 & \bar{1} & 0 \\ 0 & 0 & 1 & 0 & 0 & 0 \\ 1 & 0 & 0 & 0 & 0 & 0 \end{pmatrix}_D,$$

$$\Gamma(\gamma) = \begin{pmatrix} \bar{1} & 0 & 0 & 0 & 0 & 0 \\ 0 & \bar{1} & 0 & 0 & 0 & 0 \\ 0 & 0 & \bar{1} & 0 & 0 & 0 \\ 0 & 0 & 0 & \bar{1} & 0 & 0 \\ 0 & 0 & 0 & 0 & \bar{1} & 0 \\ 0 & 0 & 0 & 0 & 0 & \bar{1} \end{pmatrix}_D.$$

Block-diagonalization of these reducible symmetry matrices decomposes them into non-equivalent irreducible representations. These can be assigned to the two orthogonal subspaces forming the 6D embedding space $\mathbf{V} = \mathbf{V}^{\parallel} \oplus \mathbf{V}^{\perp}$, the 3D parallel (physical) subspace $\mathbf{V}^{\parallel}$ and the perpendicular 3D subspace $\mathbf{V}^{\perp}$. Thus, using $W\Gamma W^{-1} = \Gamma^{\rm red} = \Gamma^{\parallel} \oplus \Gamma^{\perp}$, we obtain

$$\Gamma(\alpha) = \left(\begin{array}{ccc|ccc} \cos(2\pi/5) & -\sin(2\pi/5) & 0 & 0 & 0 & 0 \\ \sin(2\pi/5) & \cos(2\pi/5) & 0 & 0 & 0 & 0 \\ 0 & 0 & 1 & 0 & 0 & 0 \\ \hline 0 & 0 & 0 & \cos(4\pi/5) & -\sin(4\pi/5) & 0 \\ 0 & 0 & 0 & \sin(4\pi/5) & \cos(4\pi/5) & 0 \\ 0 & 0 & 0 & 0 & 0 & 1 \end{array}\right)_V = \left(\begin{array}{c|c} \Gamma^{\parallel} & 0 \\ \hline 0 & \Gamma^{\perp} \end{array}\right)_V,$$

where

$$W = a^* \begin{pmatrix} 0 & sc4 & sc6 & sc8 & s & sc2 \\ 0 & ss4 & ss6 & ss8 & 0 & ss2 \\ 1 & c & c & c & c & c \\ \hline 0 & -sc8 & -sc2 & -sc6 & -s & -sc4 \\ 0 & -ss8 & -ss2 & -ss6 & 0 & -ss4 \\ 1 & -c & -c & -c & -c & -c \end{pmatrix}_V,$$

$c = \cos\theta$, $s = \sin\theta$, $scn = \sin\theta\cos(n\pi/5)$, $ssn = \sin\theta\sin(n\pi/5)$. The column vectors of the matrix W give the parallel- (above the partition line) and perpendicular-space components (below the partition line) of a reciprocal basis in $\mathbf{V}$. Thus, W can be rewritten using the physical-space reciprocal basis defined above and an arbitrary constant c,

$$W = \begin{pmatrix} \mathbf{a}_1^* & \mathbf{a}_2^* & \mathbf{a}_3^* & \mathbf{a}_4^* & \mathbf{a}_5^* & \mathbf{a}_6^* \\ c\mathbf{a}_1^* & -c\mathbf{a}_4^* & -c\mathbf{a}_6^* & -c\mathbf{a}_3^* & -c\mathbf{a}_5^* & -c\mathbf{a}_2^* \end{pmatrix} = \begin{pmatrix} \mathbf{d}_1^* & \mathbf{d}_2^* & \mathbf{d}_3^* & \mathbf{d}_4^* & \mathbf{d}_5^* & \mathbf{d}_6^* \end{pmatrix},$$

yielding the reciprocal basis $\mathbf{d}_i^*, i = 1, \ldots, 6$, in the 6D embedding space (D space)

$$\mathbf{d}_1^* = a^* \begin{pmatrix} 0 \\ 0 \\ 1 \\ 0 \\ 0 \\ c \end{pmatrix} \text{ and } \mathbf{d}_i^* = a^* \begin{pmatrix} \sin\theta\cos(2\pi i/5) \\ \sin\theta\sin(2\pi i/5) \\ \cos\theta \\ -c\sin\theta\cos(4\pi i/5) \\ -c\sin\theta\sin(4\pi i/5) \\ -c\cos\theta \end{pmatrix}, i = 2, \ldots, 6.$$

The 6×6 symmetry matrices can each be decomposed into two 3×3 matrices. The first one, $\Gamma^{\parallel}$, acts on the parallel-space component, the second one, $\Gamma^{\perp}$, on the perpendicular-space component. In the case of $\Gamma(\alpha)$, the coupling factor between a rotation in parallel and perpendicular space is 2. Thus a $2\pi/5$ rotation in physical space is related to a $4\pi/5$ rotation in perpendicular space (Figs. 4.6.3.28 and 4.6.3.29).

With the condition $\mathbf{d}_i \cdot \mathbf{d}_j^* = \delta_{ij}$, the basis in direct 6D space is obtained:

$$\mathbf{d}_1 = \frac{1}{2a^*} \begin{pmatrix} 0 \\ 0 \\ 1 \\ 0 \\ 0 \\ 1/c \end{pmatrix} \text{ and } \mathbf{d}_i = \frac{1}{2a^*} \begin{pmatrix} \sin\theta\cos(2\pi i/5) \\ \sin\theta\sin(2\pi i/5) \\ \cos\theta \\ -(1/c)\sin\theta\cos(4\pi i/5) \\ -(1/c)\sin\theta\sin(4\pi i/5) \\ -(1/c)\cos\theta \end{pmatrix}, \quad i = 2, \ldots, 6.$$

The metric tensors G, G^* are of the type

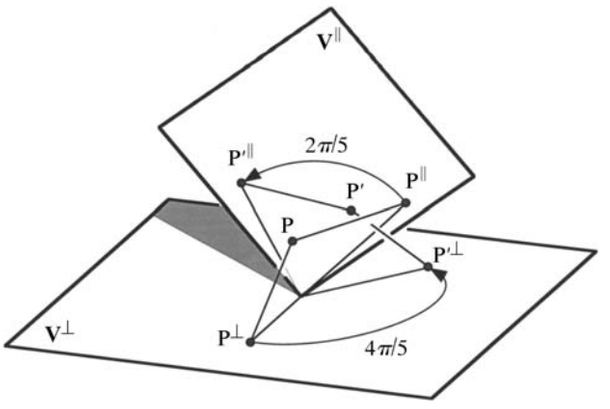

Fig. 4.6.3.29. Schematic representation of a rotation in 6D space. The point P is rotated to P′. The component rotations in parallel and perpendicular space are illustrated.

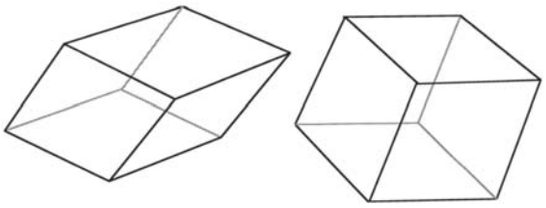

Fig. 4.6.3.30. The two unit tiles of the 3D Penrose tiling: a prolate [$\alpha_p = \arccos(5^{-1/2}) \simeq 63.44^\circ$] and an oblate ($\alpha_o = 180^\circ - \alpha_p$) rhombohedron with equal edge lengths a_r.

$$\begin{pmatrix} A & B & B & B & B & B \\ B & A & B & -B & -B & B \\ B & B & A & B & -B & -B \\ B & -B & B & A & B & -B \\ B & -B & -B & B & A & B \\ B & B & -B & -B & B & A \end{pmatrix},$$

with $A = (1 + c^2)a^{*2}$, $B = [(5)^{1/2}/5](1 - c^2)a^{*2}$ for the reciprocal space and $A = (1 + c^2)/[4(ca^*)^2]$, $B = [(5)^{1/2}(c^2 - 1)]/[20(ca^*)^2]$ for the direct space. For $c = 1$ we obtain hypercubic direct and reciprocal 6D lattices.

The lattice parameters in reciprocal and direct space are $d_i^* = a^*(2)^{1/2}$ and $d_i = 1/[(2)^{1/2}a^*]$ with $i = 1, \ldots, 6$, respectively. The volume of the 6D unit cell can be calculated from the metric tensor G. For $c = 1$ it is simply $V = [\det(G)]^{1/2} = \{1/[(2)^{1/2}a^*]\}^6$.

The best known example of a 3D quasiperiodic structure is the canonical 3D *Penrose tiling* (see Janssen, 1986). It can be constructed from two unit tiles: a prolate and an oblate rhombohedron with equal edge lengths a_r (Fig. 4.6.3.30). Each face of the rhombohedra is a rhomb with acute angles $\alpha_r = \arccos[1/(5)^{1/2}] \simeq 63.44^\circ$. Their volumes are $V_p = (4/5)a_r^3 \sin(2\pi/5)$, $V_o = (4/5)a_r^3 \sin(\pi/5) = V_p/\tau$, and their frequencies $\nu_p{:}\nu_o = \tau{:}1$. The resulting point density (number of vertices per unit volume) is $\rho_p = (\tau + 1)/(\tau V_p + V_o) = (\tau/a_r^3)\sin(2\pi/5)$. Ten prolate and ten oblate rhombohedra can be packed to form a rhombic triacontahedron. The icosahedral symmetry of this zonohedron is broken by the many possible decompositions into the rhombohedra. Removing one zone of the triacontahedron gives a rhomb-icosahedron consisting of five prolate and five oblate rhombohedra. Again, the singular fivefold axis of the rhomb-icosahedron is broken by the decomposition into rhombohedra. Removing one zone again gives a rhombic dodecahedron consisting of two prolate and two oblate rhombohedra. Removing the last remaining zone leads finally to a single prolate rhombohedron. Using these zonohedra as elementary clusters, a matching rule can be derived for the 3D construction of the 3D Penrose tiling (Levine & Steinhardt, 1986; Socolar & Steinhardt, 1986).

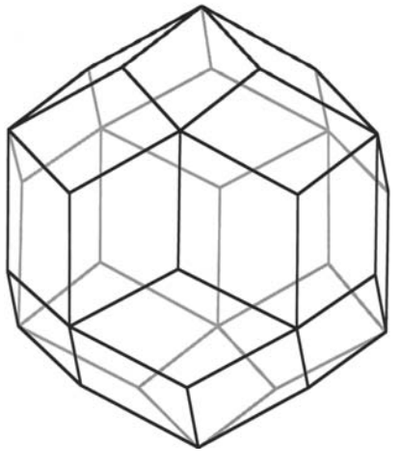

Fig. 4.6.3.31. Atomic surface of the 3D Penrose tiling in the 6D hypercubic description. The projection of the 6D hypercubic unit cell upon $\mathbf{V}^\perp$ gives a rhombic triacontahedron.

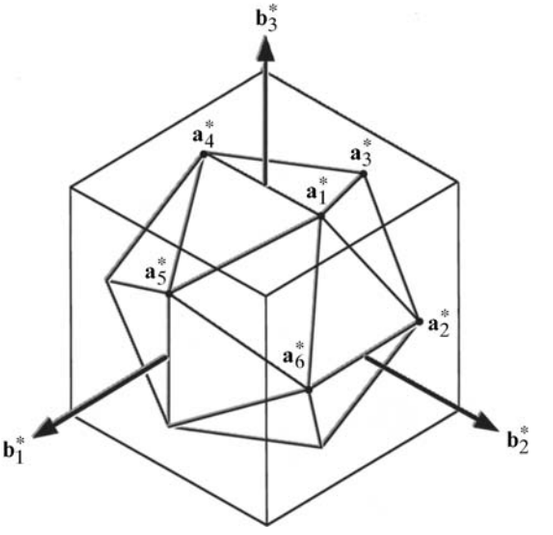

Fig. 4.6.3.32. Perspective parallel-space view of the two alternative reciprocal bases of the 3D Penrose tiling: the cubic and the icosahedral setting, represented by the bases $\mathbf{b}_i^*$, $i = 1, \ldots, 3$, and $\mathbf{a}_i^*$, $i = 1, \ldots, 6$, respectively.

The 3D Penrose tiling can be embedded in the 6D space as shown above. The 6D hypercubic lattice is decorated on the lattice nodes with 3D triacontahedra obtained from the projection of a 6D unit cell upon the perpendicular space $\mathbf{V}^\perp$ (Fig. 4.6.3.31). Thus the edge length of the rhombs covering the triacontahedron is equivalent to the length $\pi^\perp(\mathbf{d}_i) = 1/2a^*$ of the perpendicular-space component of the vectors spanning the 6D hypercubic lattice $\Sigma = \{\mathbf{r} = \sum_{i=1}^6 n_i\mathbf{d}_i | n_i \in \mathbb{Z}\}$.

4.6.3.3.3.1. Indexing

There are several indexing schemes in use. The generic one uses a set of six rationally independent reciprocal-basis vectors pointing to the corners of an icosahedron, $\mathbf{a}_1^* = a^*(0, 0, 1)$, $\mathbf{a}_i^* = a^*[\sin\theta\cos(2\pi i/5), \sin\theta\sin(2\pi i/5), \cos\theta]$, $i = 2, \ldots, 6$, $\sin\theta = 2/(5)^{1/2}$, $\cos\theta = 1/(5)^{1/2}$, with $\theta \simeq 63.44^\circ$, the angle between two neighbouring fivefold axes (setting 1) (Fig. 4.6.3.28). In this case, the physical-space basis corresponds to a simple projection of the 6D reciprocal basis $\mathbf{d}_i^*$, $i = 1, \ldots, 6$. Sometimes, the same set of six reciprocal-basis vectors is referred to a differently oriented Cartesian reference system (C basis, with basis vectors $\mathbf{e}_i$ along the twofold axes) (Bancel *et al.*, 1985). The reciprocal basis is

$$\begin{pmatrix} \mathbf{a}_1^* \\ \mathbf{a}_2^* \\ \mathbf{a}_3^* \\ \mathbf{a}_4^* \\ \mathbf{a}_5^* \\ \mathbf{a}_6^* \end{pmatrix} = \frac{a^*}{(1+\tau^2)^{1/2}} \begin{pmatrix} 0 & 1 & \tau \\ -1 & \tau & 0 \\ -\tau & 0 & 1 \\ 0 & -1 & \tau \\ \tau & 0 & 1 \\ 1 & \tau & 0 \end{pmatrix}_C \begin{pmatrix} \mathbf{e}_1^C \\ \mathbf{e}_2^C \\ \mathbf{e}_3^C \end{pmatrix}.$$

An alternate way of indexing is based on a 3D set of cubic reciprocal-basis vectors $\mathbf{b}_i^*$, $i = 1, \ldots, 3$ (setting 2) (Fig. 4.6.3.32):

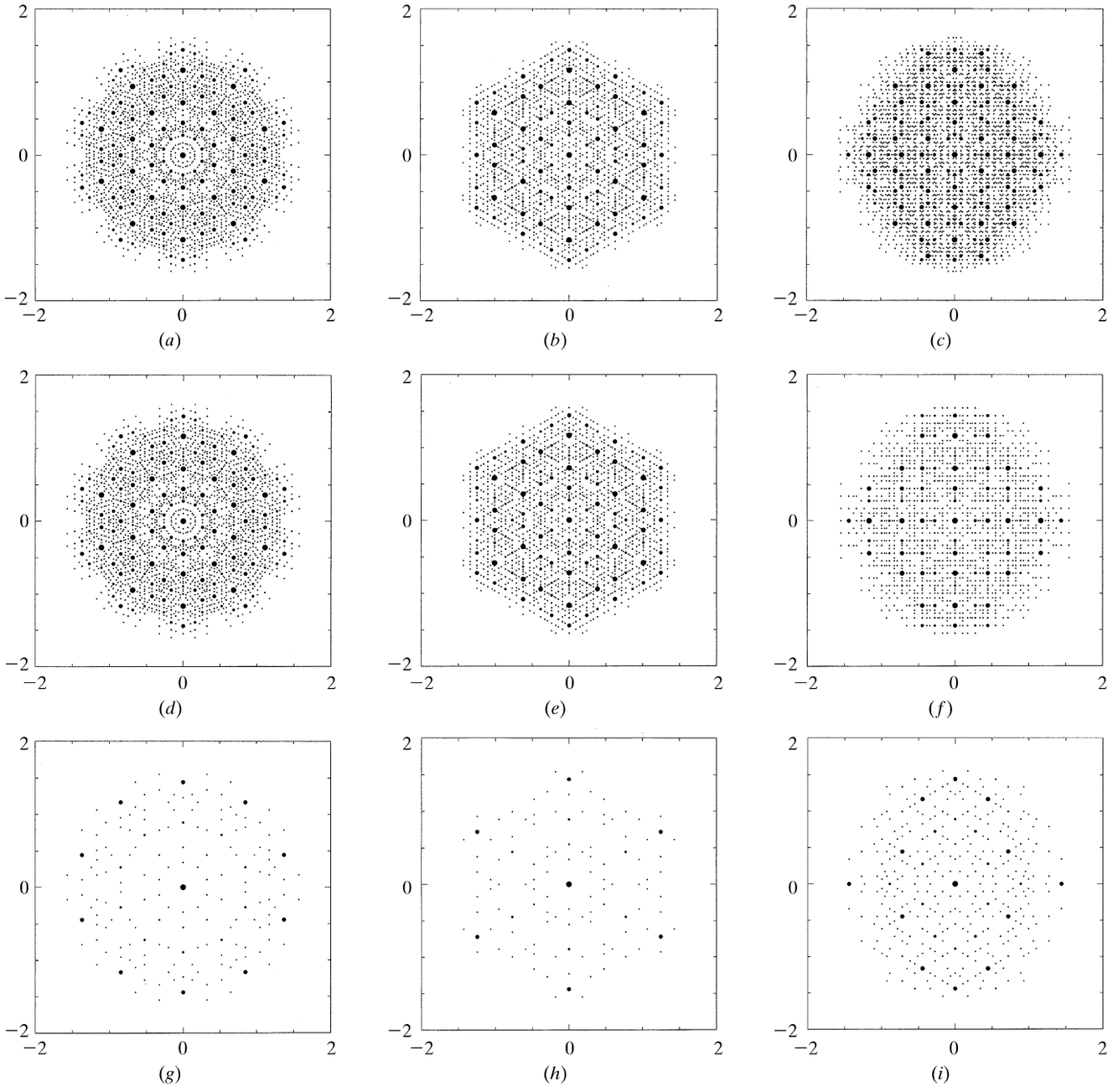

Fig. 4.6.3.33. Physical-space diffraction patterns of the 3D Penrose tiling decorated with point atoms (edge lengths of the Penrose unit rhombohedra $a_r = 5.0$ Å). Sections with five-, three- and twofold symmetry are shown for the primitive 6D analogue of Bravais type P in (a, b, c), the body-centred 6D analogue to Bravais type I in (d, e, f) and the face-centred 6D analogue to Bravais type F in (g, h, i). All reflections are shown within $10^{-4}|F(\mathbf{0})|^2 < |F(\mathbf{H})|^2 < |F(\mathbf{0})|^2$ and $-6 \le h_i \le 6, i = 1, \ldots, 6$.

$$\begin{pmatrix} \mathbf{b}_1^* \\ \mathbf{b}_2^* \\ \mathbf{b}_3^* \end{pmatrix} = \tfrac{1}{2}\begin{pmatrix} 0 & \bar{1} & 0 & 0 & 0 & 1 \\ 1 & 0 & 0 & \bar{1} & 0 & 0 \\ 0 & 0 & 1 & 0 & 1 & 0 \end{pmatrix}_D \begin{pmatrix} \mathbf{a}_1^* \\ \mathbf{a}_2^* \\ \mathbf{a}_3^* \\ \mathbf{a}_4^* \\ \mathbf{a}_5^* \\ \mathbf{a}_6^* \end{pmatrix}$$

$$= \frac{a^*}{(1+\tau^2)^{1/2}} \begin{pmatrix} \mathbf{e}_1^C \\ \mathbf{e}_2^C \\ \mathbf{e}_3^C \end{pmatrix}.$$

The Cartesian C basis is related to the V basis by a $\theta/2$ rotation around $[100]_C$, yielding $[001]_V$, followed by a $\pi/10$ rotation around $[001]_C$:

$$\begin{pmatrix} \mathbf{e}_1^C \\ \mathbf{e}_2^C \\ \mathbf{e}_3^C \end{pmatrix} = \begin{pmatrix} \cos(\pi/10) & \sin(\pi/10) & 0 \\ -\cos(\theta/2)\sin(\pi/10) & \cos(\theta/2)\cos(\pi/10) & \sin(\theta/2) \\ \sin(\theta/2)\sin(\pi/10) & -\sin(\theta/2)\cos(\pi/10) & \cos(\theta/2) \end{pmatrix}_V \begin{pmatrix} \mathbf{e}_1^V \\ \mathbf{e}_2^V \\ \mathbf{e}_3^V \end{pmatrix}.$$

Thus, indexing the diffraction pattern of an icosahedral phase with integer indices, one obtains for setting 1 $\mathbf{H} = \sum_{i=1}^{6} h_i \mathbf{a}_i^*, h_i \in \mathbb{Z}$. These indices $(h_1\ h_2\ h_3\ h_4\ h_5\ h_6)$ transform into the second setting to $(h/h'\ k/k'\ l/l')$ with the fractional cubic indices $h_1^c = h + h'\tau$, $h_2^c = k + k'\tau$, $h_3^c = l + l'\tau$. The transformation matrix is

Table 4.6.3.2. *3D point groups of order k describing the diffraction symmetry and corresponding 6D decagonal space groups with reflection conditions (see Levitov & Rhyner, 1988; Rokhsar et al., 1988)*

3D point group	k	5D space group	Reflection condition
$\frac{2}{m}\bar{3}\bar{5}$	120	$P\frac{2}{m}\bar{3}\bar{5}$	No condition
		$P\frac{2}{n}\bar{3}\bar{5}$	$h_1h_2\overline{h_1h_2}h_5h_6$: $h_5 - h_6 = 2n$
		$I\frac{2}{m}\bar{3}\bar{5}$	$h_1h_2h_3h_4h_5h_6$: $\sum_{i=1}^{6} h_i = 2n$
		$F\frac{2}{m}\bar{3}\bar{5}$	$h_1h_2h_3h_4h_5h_6$: $\sum_{i\neq j=1}^{6} h_i + h_j = 2n$
		$F\frac{2}{n}\bar{3}\bar{5}$	$h_1h_2h_3h_4h_5h_6$: $\sum_{i\neq j=1}^{6} h_i + h_j = 2n$ $h_1h_2\overline{h_1h_2}h_5h_6$: $h_5 - h_6 = 4n$
235	60	$P235$	No condition
		$P235_1$	$h_1h_2h_2h_2h_2h_2$: $h_1 = 5n$
		$I235$	$h_1h_2h_3h_4h_5h_6$: $\sum_{i=1}^{6} h_i = 2n$
		$I235_1$	$h_1h_2h_3h_4h_5h_6$: $\sum_{i=1}^{6} h_i = 2n$ $h_1h_2h_2h_2h_2h_2$: $h_1 + 5h_2 = 10n$
		$F235$	$h_1h_2h_3h_4h_5h_6$: $\sum_{i\neq j=1}^{6} h_i + h_j = 2n$
		$F235_1$	$h_1h_2h_3h_4h_5h_6$: $\sum_{i\neq j=1}^{6} h_i + h_j = 2n$ $h_1h_2h_2h_2h_2h_2$: $h_1 + 5h_2 = 10n$

$$\begin{pmatrix} h \\ h' \\ k \\ k' \\ l \\ l' \end{pmatrix}_C = \begin{pmatrix} 0 & \bar{1} & 0 & 0 & 0 & 1 \\ 0 & 0 & \bar{1} & 0 & 1 & 0 \\ 1 & 0 & 0 & \bar{1} & 0 & 0 \\ 0 & 1 & 0 & 0 & 0 & 1 \\ 0 & 0 & 1 & 0 & 1 & 0 \\ 1 & 0 & 0 & 1 & 0 & 0 \end{pmatrix} \begin{pmatrix} h_1 \\ h_2 \\ h_3 \\ h_4 \\ h_5 \\ h_6 \end{pmatrix}_D = \begin{pmatrix} h_6 - h_2 \\ h_5 - h_3 \\ h_1 - h_4 \\ h_6 + h_2 \\ h_5 + h_3 \\ h_1 + h_4 \end{pmatrix}_D .$$

4.6.3.3.3.2. Diffraction symmetry

The diffraction symmetry of icosahedral phases can be described by the Laue group $K = m\bar{3}\bar{5}$. The set of all vectors $\mathbf{H}$ forms a Fourier module $M^* = \{\mathbf{H}^{\parallel} = \sum_{i=1}^{6} h_i \mathbf{a}_i^* | h_i \in \mathbb{Z}\}$ of rank 6 in physical space. Consequently, it can be considered as a projection from a 6D reciprocal lattice, $M^* = \pi^{\parallel}(\Sigma^*)$. The parallel and perpendicular reciprocal-space sections of the 3D Penrose tiling decorated with equal point scatterers on its vertices are shown in Figs. 4.6.3.33 and 4.6.3.34. The diffraction pattern in perpendicular space is the Fourier transform of the triacontahedron. All Bragg reflections within $10^{-4}|F(\mathbf{0})|^2 < |F(\mathbf{H})|^2 < |F(\mathbf{0})|^2$ are depicted. Without intensity-truncation limit, the diffraction pattern would be densely filled with discrete Bragg reflections.

The 6D icosahedral space groups that are relevant to the description of icosahedral phases (six symmorphous and five non-symmorphous groups) are listed in Table 4.6.3.2. These space groups are a subset of all 6D icosahedral space groups fulfilling the condition that the 6D point groups they are associated with are isomorphous to the 3D point groups $\frac{2}{m}\bar{3}\bar{5}$ and 235 describing the diffraction symmetry. From 826 6D (analogues to) Bravais groups (Levitov & Rhyner, 1988), only three fulfil the condition that the projection of the 6D hypercubic lattice upon the 3D physical space is compatible with the icosahedral point groups $\frac{2}{m}\bar{3}\bar{5}$, 235: the primitive hypercubic Bravais lattice P, the body-centred Bravais lattice I with translation 1/2(111111), and the face-centred Bravais lattice F with translations 1/2(110000) + 14 further cyclic permutations. Hence, the I lattice is twofold primitive (*i.e.* it contains two vertices per unit cell) and the F lattice is 16-fold primitive. The orientation of the symmetry elements in the 6D space is defined by the isomorphism of the 3D and 6D point groups. The action of the fivefold rotation, however, is different in the subspaces $\mathbf{V}^{\parallel}$ and $\mathbf{V}^{\perp}$: a rotation of $2\pi/5$ in $\mathbf{V}^{\parallel}$ is correlated with a rotation of $4\pi/5$ in $\mathbf{V}^{\perp}$. The reflection and inversion operations are equivalent in both subspaces.

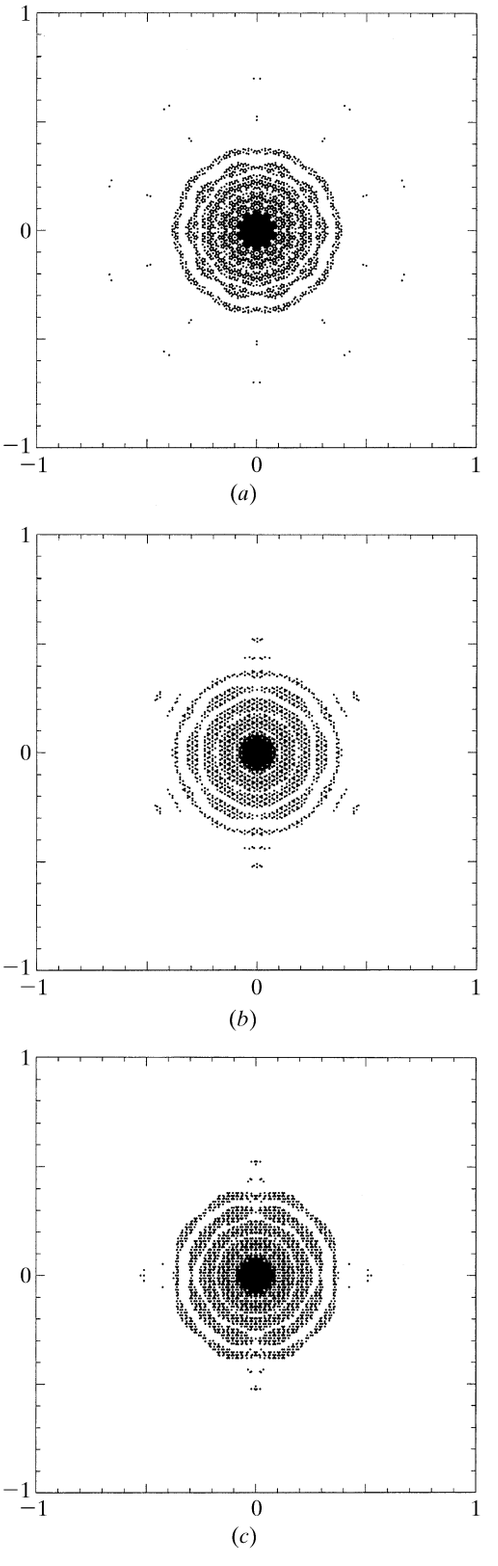

Fig. 4.6.3.34. Perpendicular-space diffraction patterns of the 3D Penrose tiling decorated with point atoms (edge lengths of the Penrose unit rhombohedra a_r = 5.0 Å). Sections with (*a*) five-, (*b*) three- and (*c*) twofold symmetry are shown for the primitive 6D analogue of Bravais type P. All reflections are shown within $10^{-4}|F(\mathbf{0})|^2 < |F(\mathbf{H})|^2 < |F(\mathbf{0})|^2$ and $-6 \leq h_i \leq 6, i = 1, \ldots, 6$.

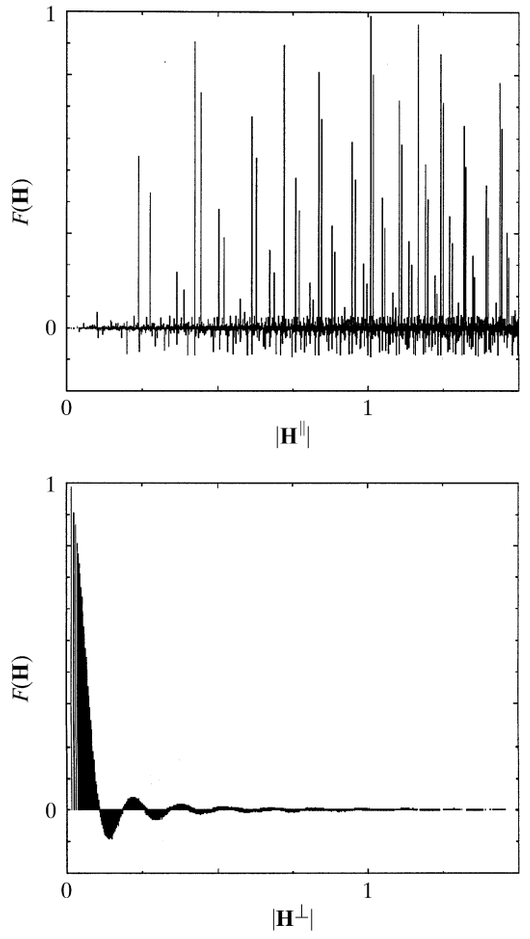

Fig. 4.6.3.35. Radial distribution function of the structure factors $F(\mathbf{H})$ of the 3D Penrose tiling (edge lengths of the Penrose unit rhombohedra $a_r = 5.0$ Å) decorated with point atoms as a function of $|\mathbf{H}^{\parallel}|$ (above) and $|\mathbf{H}^{\perp}|$ (below). All reflections are shown within $10^{-6}|F(\mathbf{0})|^2 < |F(\mathbf{H})|^2 < |F(\mathbf{0})|^2$ and $-6 \le h_i \le 6, i = 1, \ldots, 6$.

4.6.3.3.3.3. Structure factor

The structure factor of the icosahedral phase corresponds to the Fourier transform of the 6D unit cell,

$$F(\mathbf{H}) = \sum_{k=1}^{N} f_k(\mathbf{H}^{\parallel}) T_k(\mathbf{H}^{\parallel}, \mathbf{H}^{\perp}) g_k(\mathbf{H}^{\perp}) \exp(2\pi i \mathbf{H} \cdot \mathbf{r}_k),$$

with 6D diffraction vectors $\mathbf{H} = \sum_{i=1}^{6} h_i \mathbf{d}_i^*$, parallel-space atomic scattering factor $f_k(H^{\parallel})$, temperature factor $T_k(\mathbf{H}^{\parallel}, \mathbf{H}^{\perp})$ and perpendicular-space geometric form factor $g_k(\mathbf{H}^{\perp})$. $T_k(\mathbf{H}^{\parallel}, \mathbf{0})$ is equivalent to the conventional Debye–Waller factor and $T_k(\mathbf{0}, \mathbf{H}^{\perp})$ describes random fluctuations in perpendicular space. These fluctuations cause characteristic jumps of vertices (*phason flips*) in the physical space. Even random phason flips map the vertices onto positions that can still be described by physical-space vectors of the type $\mathbf{r} = \sum_{i=1}^{6} n_i \mathbf{a}_i$. Consequently, the set $M = \{\mathbf{r} = \sum_{i=1}^{6} n_i \mathbf{a}_i | n_i \in \mathbb{Z}\}$ of all possible vectors forms a $\mathbb{Z}$ module. The shape of the atomic surfaces corresponds to a selection rule for the positions actually occupied. The geometric form factor $g_k(\mathbf{H}^{\perp})$ is equivalent to the Fourier transform of the *atomic surface*, *i.e.* the 3D perpendicular-space component of the 6D *hyperatoms*.

For the example of the canonical 3D Penrose tiling, $g_k(\mathbf{H}^{\perp})$ corresponds to the Fourier transform of a triacontahedron:

$$g_k(\mathbf{H}^{\perp}) = (1/A_{\mathrm{UC}}^{\perp}) \int_{A_k} \exp(2\pi i \mathbf{H}^{\perp} \cdot \mathbf{r})\, \mathrm{d}\mathbf{r},$$

where $A_{\mathrm{UC}}^{\perp}$ is the volume of the 6D unit cell projected upon $\mathbf{V}^{\perp}$ and A_k is the volume of the triacontahedron. $A_{\mathrm{UC}}^{\perp}$ and A_k are equal in the present case and amount to the volumes of ten prolate and ten oblate rhombohedra: $A_{\mathrm{UC}}^{\perp} = 8a_r^3[\sin(2\pi/5) + \sin(\pi/5)]$. Evaluating the integral by decomposing the triacontahedron into trigonal pyramids, each one directed from the centre of the triacontahedron to three of its corners given by the vectors $\mathbf{e}_i$, $i = 1, \ldots, 3$, one obtains

$$g(\mathbf{H}^{\perp}) = (1/A_{\mathrm{UC}}^{\perp}) \sum_{R} g_k(R^T \mathbf{H}^{\perp}),$$

with $k = 1, \ldots, 60$ running over all site-symmetry operations R of the icosahedral group,

$$\begin{aligned} g_k(\mathbf{H}^{\perp}) = -iV_r[&A_2A_3A_4 \exp(iA_1) + A_1A_3A_5 \exp(iA_2) \\ &+ A_1A_2A_6 \exp(iA_3) + A_4A_5A_6] \\ &\times (A_1A_2A_3A_4A_5A_6)^{-1}, \end{aligned}$$

$A_j = 2\pi \mathbf{H}^{\perp} \cdot \mathbf{e}_j$, $j = 1, \ldots, 3$, $A_4 = A_2 - A_3$, $A_5 = A_3 - A_1$, $A_6 = A_1 - A_2$ and $V_r = \mathbf{e}_1 \cdot (\mathbf{e}_2 \times \mathbf{e}_3)$ the volume of the parallelepiped defined by the vectors $\mathbf{e}_i$, $i = 1, \ldots, 3$ (Yamamoto, 1992*b*).

4.6.3.3.3.4. Intensity statistics

The radial structure-factor distributions of the 3D Penrose tiling decorated with point scatterers are plotted in Fig. 4.6.3.35 as a function of parallel and perpendicular space. The distribution of $|F(\mathbf{H})|$ as a function of their frequencies clearly resembles a centric distribution, as can be expected from the centrosymmetric unit cell. The shape of the distribution function depends on the radius of the limiting sphere in reciprocal space. The number of weak reflections increases as the power 6, that of strong reflections only as the power 3 (strong reflections always have small $\mathbf{H}^{\perp}$ components).

The weighted reciprocal space of the 3D Penrose tiling contains an infinite number of Bragg reflections within a limited region of the physical space. Contrary to the diffraction pattern of a periodic structure consisting of point atoms on the lattice nodes, the Bragg reflections show intensities depending on the perpendicular-space components of their diffraction vectors.

4.6.3.3.3.5. Relationships between structure factors at symmetry-related points of the Fourier image

The weighted 3D reciprocal space $M^* = \{\mathbf{H}^{\parallel} = \sum_{i=1}^{6} h_i \mathbf{a}_i^* | h_i \in \mathbb{Z}\}$ exhibits the icosahedral point symmetry $K = m\bar{3}5$. It is invariant under the action of the scaling matrix S^3:

$$S = \tfrac{1}{2}\begin{pmatrix} 1 & 1 & 1 & 1 & 1 & 1 \\ 1 & 1 & 1 & -1 & -1 & 1 \\ 1 & 1 & 1 & 1 & -1 & -1 \\ 1 & -1 & 1 & 1 & 1 & -1 \\ 1 & -1 & -1 & 1 & 1 & 1 \\ 1 & 1 & -1 & -1 & 1 & 1 \end{pmatrix}_D, \quad S^3 = \begin{pmatrix} 2 & 1 & 1 & 1 & 1 & 1 \\ 1 & 2 & 1 & -1 & -1 & 1 \\ 1 & 1 & 2 & 1 & -1 & -1 \\ 1 & -1 & 1 & 2 & 1 & -1 \\ 1 & -1 & -1 & 1 & 2 & 1 \\ 1 & 1 & -1 & -1 & 1 & 2 \end{pmatrix}_D,$$

$$\begin{pmatrix} 2 & 1 & 1 & 1 & 1 & 1 \\ 1 & 2 & 1 & -1 & -1 & 1 \\ 1 & 1 & 2 & 1 & -1 & -1 \\ 1 & -1 & 1 & 2 & 1 & -1 \\ 1 & -1 & -1 & 1 & 2 & 1 \\ 1 & 1 & -1 & -1 & 1 & 2 \end{pmatrix}_D \begin{pmatrix} \mathbf{a}_1^* \\ \mathbf{a}_2^* \\ \mathbf{a}_3^* \\ \mathbf{a}_4^* \\ \mathbf{a}_5^* \\ \mathbf{a}_6^* \end{pmatrix} = \tau^3 \begin{pmatrix} \mathbf{a}_1^* \\ \mathbf{a}_2^* \\ \mathbf{a}_3^* \\ \mathbf{a}_4^* \\ \mathbf{a}_5^* \\ \mathbf{a}_6^* \end{pmatrix}.$$

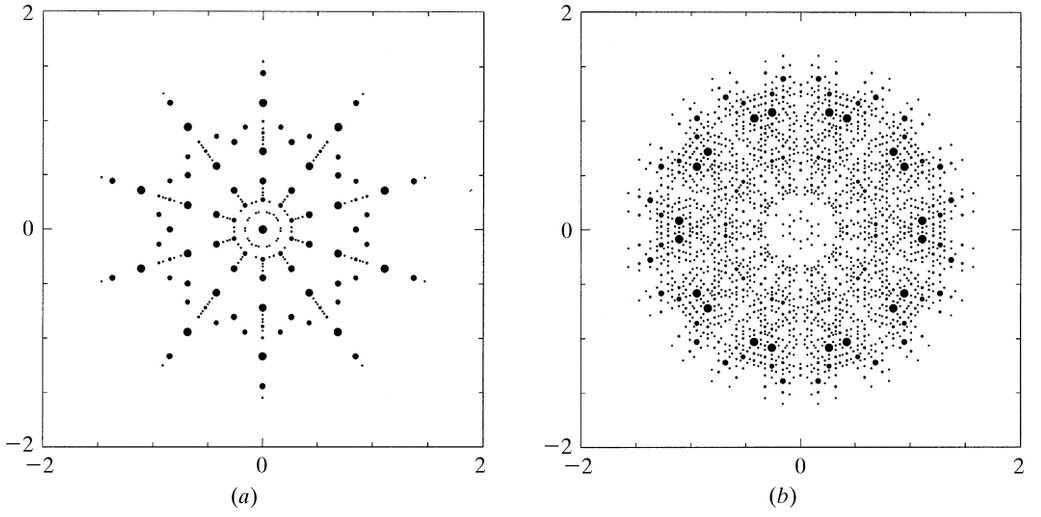

Fig. 4.6.3.36. Parallel-space distribution of (*a*) positive and (*b*) negative structure factors of the 3D Penrose tiling of the 6D *P* lattice type decorated with point atoms (edge lengths of the Penrose unit rhombohedra a_r = 5.0 Å). The magnitudes of the structure factors are indicated by the diameters of the filled circles. All reflections are shown within $10^{-4}|F(\mathbf{0})|^2 < |F(\mathbf{H})|^2 < |F(\mathbf{0})|^2$ and $-6 \le h_i \le 6, i = 1, \ldots, 6$.

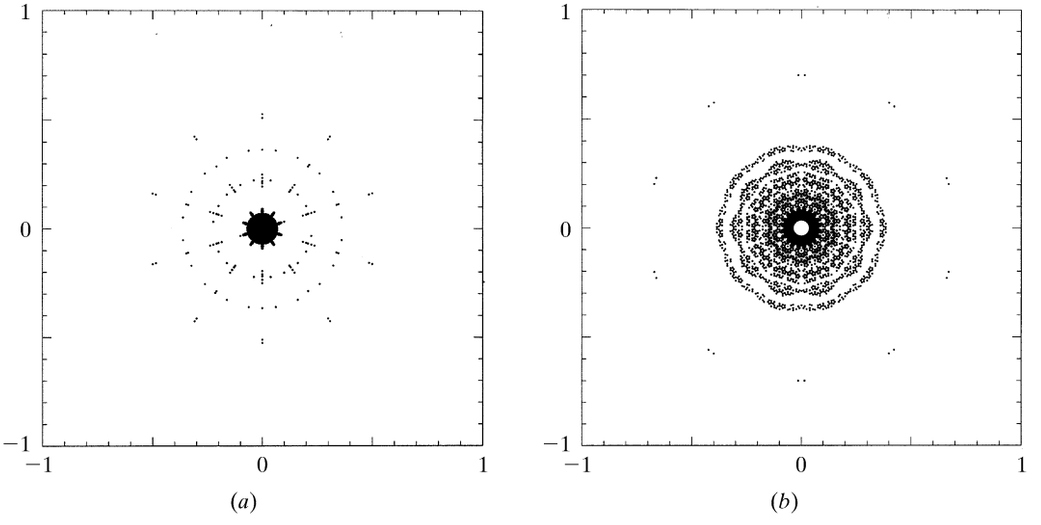

Fig. 4.6.3.37. Perpendicular-space distribution of (*a*) positive and (*b*) negative structure factors of the 3D Penrose tiling of the 6D *P* lattice type decorated with point atoms (edge lengths of the Penrose unit rhombohedra a_r = 5.0 Å). The magnitudes of the structure factors are indicated by the diameters of the filled circles. All reflections are shown within $10^{-4}|F(\mathbf{0})|^2 < |F(\mathbf{H})|^2 < |F(\mathbf{0})|^2$ and $-6 \le h_i \le 6, i = 1, \ldots, 6$.

Table 4.6.4.1. *Intensity statistics of the Fibonacci chain for a total of 161 322 reflections with* $-1000 \le h_i \le 1000$ *and* $0 \le \sin\theta/\lambda \le 2$ Å^{-1}

In the upper line, the number of reflections in the respective interval is given; in the lower line the partial sums $\sum I(\mathbf{H})$ of the intensities $I(\mathbf{H})$ are given as a percentage of the total diffracted intensity. The $F(00)$ reflection is not included in the sums.

	$F(\mathbf{H})/F(\mathbf{H})_{max} \ge 0.1$	$0.1 > F(\mathbf{H})/F(\mathbf{H})_{max} \ge 0.01$	$0.01 > F(\mathbf{H})/F(\mathbf{H})_{max} \ge 0.001$	$F(\mathbf{H})/F(\mathbf{H})_{max} < 0.001$
$0 \le \sin\theta/\lambda \le 0.2$ Å^{-1}	17	148	1505	14 511
$\sum I(\mathbf{H})$	52.53%	2.56%	0.27%	0.03%
$0.2 \le \sin\theta/\lambda \le 0.4$ Å^{-1}	11	107	1066	14 998
$\sum I(\mathbf{H})$	27.03%	2.03%	0.19%	0.02%
$0.4 \le \sin\theta/\lambda \le 0.6$ Å^{-1}	9	64	654	15 456
$\sum I(\mathbf{H})$	9.84%	0.96%	0.12%	0.01%
$0.6 \le \sin\theta/\lambda \le 0.8$ Å^{-1}	6	27	326	15 823
$\sum I(\mathbf{H})$	2.94%	0.34%	0.07%	0.01%
$0.8 \le \sin\theta/\lambda \le 2$ Å^{-1}	1	35	338	96 720
$\sum I(\mathbf{H})$	0.23%	0.79%	0.06%	0.01%
Total sum	44	381	3389	157 508
	92.57%	6.67%	0.70%	0.06%

The scaling transformation $(S^{-3})^T$ leaves a primitive 6D reciprocal lattice invariant as can easily be seen from its application on the indices:

$$\begin{pmatrix} h_1' \\ h_2' \\ h_3' \\ h_4' \\ h_5' \\ h_6' \end{pmatrix} = \begin{pmatrix} -2 & 1 & 1 & 1 & 1 & 1 \\ 1 & -2 & 1 & -1 & -1 & 1 \\ 1 & 1 & -2 & 1 & -1 & -1 \\ 1 & -1 & 1 & -2 & 1 & -1 \\ 1 & -1 & -1 & 1 & -2 & 1 \\ 1 & 1 & -1 & -1 & 1 & -2 \end{pmatrix}_D \begin{pmatrix} h_1 \\ h_2 \\ h_3 \\ h_4 \\ h_5 \\ h_6 \end{pmatrix}.$$

The matrix $(S^{-1})^T$ leaves $M^* = \{\mathbf{H}^{\parallel} = \sum_{i=1}^{6} h_i \mathbf{a}_i^* | h_i \in \mathbb{Z}\}$ invariant,

$$\begin{pmatrix} h_1' \\ h_2' \\ h_3' \\ h_4' \\ h_5' \\ h_6' \end{pmatrix} = \tfrac{1}{2}\begin{pmatrix} -1 & 1 & 1 & 1 & 1 & 1 \\ 1 & -1 & 1 & -1 & -1 & 1 \\ 1 & 1 & -1 & 1 & -1 & -1 \\ 1 & -1 & 1 & -1 & 1 & -1 \\ 1 & -1 & -1 & 1 & -1 & 1 \\ 1 & 1 & -1 & -1 & 1 & -1 \end{pmatrix}_D \begin{pmatrix} h_1 \\ h_2 \\ h_3 \\ h_4 \\ h_5 \\ h_6 \end{pmatrix},$$

for any $\mathbf{H} = \sum_{i=1}^{6} h_i \mathbf{d}_i^*$ with h_i all even or all odd, corresponding to a 6D face-centred hypercubic lattice. In a second case the sum $\sum_{i=1}^{6} h_i$ is even, corresponding to a 6D body-centred hypercubic lattice. Block-diagonalization of the matrix S decomposes it into two irreducible representations. With $WSW^{-1} = S_V = S_V^{\parallel} \oplus S_V^{\perp}$ we obtain

$$S_V = \left(\begin{array}{ccc|ccc} \tau & 0 & 0 & 0 & 0 & 0 \\ 0 & \tau & 0 & 0 & 0 & 0 \\ 0 & 0 & \tau & 0 & 0 & 0 \\ \hline 0 & 0 & 0 & -1/\tau & 0 & 0 \\ 0 & 0 & 0 & 0 & -1/\tau & 0 \\ 0 & 0 & 0 & 0 & 0 & -1/\tau \end{array}\right)_V = \left(\begin{array}{c|c} S^{\parallel} & 0 \\ \hline 0 & S^{\perp} \end{array}\right)_V,$$

the scaling properties in the two 3D subspaces: scaling by a factor τ in parallel space corresponds to a scaling by a factor $(-\tau)^{-1}$ in perpendicular space. For the intensities of the scaled reflections analogous relationships are valid, as discussed for decagonal phases (Figs. 4.6.3.36 and 4.6.3.37, Section 4.6.3.3.2.5).

4.6.4. Experimental aspects of the reciprocal-space analysis of aperiodic crystals

4.6.4.1. Data-collection strategies

Theoretically, aperiodic crystals show an infinite number of reflections within a given diffraction angle, contrary to periodic crystals. The number of reflections to be included in a structure analysis of a *periodic* crystal may be very high (one million for virus crystals, for instance) but there is no ambiguity in the selection of reflections to be collected: all Bragg reflections within a limiting sphere in reciprocal space, usually given by $0 \leq \sin\theta/\lambda \leq 0.7$ Å^{-1}, are used. All reflections, observed and unobserved, are included to fit a reliable structure model.

However, for *aperiodic* crystals it is not possible to collect the infinite number of dense Bragg reflections within $0 \leq \sin\theta/\lambda \leq 0.7$ Å^{-1}. The number of observable reflections within this limiting sphere depends only on the spatial and intensity resolution.

What happens if not all reflections are included in a structure analysis? How important is the contribution of reflections with large perpendicular-space components of the diffraction vector which are weak but densely distributed? These problems are illustrated using the example of the Fibonacci sequence. An infinite model structure consisting of Al atoms with isotropic thermal parameter $B = 1$ Å^2, and distances S = 2.5 Å and L = τS, was used for the calculations (Table 4.6.4.1).

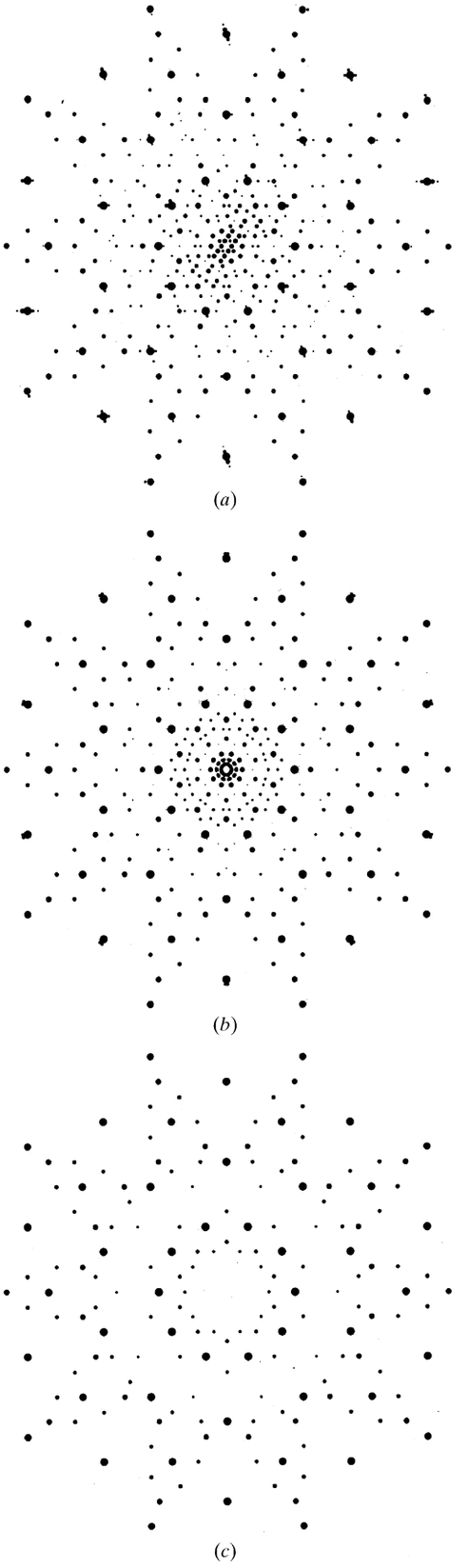

Fig. 4.6.4.1. Simulated diffraction patterns of (*a*) the $\simeq 52$ Å single-crystal approximant of decagonal Al–Co–Ni, (*b*) the fivefold twinned approximant, and (*c*) the decagonal phase itself (Estermann *et al.*, 1994).

references